# VALIDATION OF ANALYTIC MODELLING OF LOCAL REAR CONTACTS IN PERC/PERL SOLAR CELLS

Pierre Saint-Cast, Nico Wöhrle, Johannes Greulich
Fraunhofer Institute for Solar Energy Systems ISE
Heidenhofstraße 2, 79110 Freiburg, Germany

ABSTRACT: This work focuses on the comparison of analytical modelling of local rear contacts with two- and three-dimensional (2D and 3D) numerical simulation. The analytical models were developed to calculate the effective surface recombination velocity ($S_{eff}$) of the rear surface and the bulk contribution to the series resistance ($R_{S\_rear}$). These parameters represent an effective rear surface and when combined to a one-dimensional (1D) simulation can be used to model the current-voltage characteristics of the solar cell. The first achievement of this paper is a solid comparison of the analytical model and the numerical simulation. The deviation is found to be lower than 20% for more than 95% of the data reported. However the model of $S_{eff}$ is found to be limited to open circuit (OC) condition. Therefore a correction, which extended the validity range of the $S_{eff}$ calculation to maximum power point (MPP) condition, is proposed without loss of accuracy. The last achievement is the comparison of the efficiencies obtained using the 1D simulation with the ones obtained using the 2D and 3D numerical simulation. This method ensures with 95% confidence that the deviation in efficiency will not exceed ± 0.18%$_{abs}$ for point contact and ± 0.28%$_{abs}$ for line contacts.

Keywords: Analytical modelling; Simulation; PERC

## 1 INTRODUCTION

"Passivated Emitter and Rear Cell" (PERC, [1]) technology is quickly spreading out in crystalline silicon photovoltaics, becoming the industry standard for the next decades. The structuring of the rear of solar cells poses the problem of trade-offs between high rear surface recombination and low series resistance with its mutual variable being contact distance. So far, the theoretical models proposed have been focusing on finding the optimal contact geometry for one given contact technology [2-10]. Most of the simple models [2-4, 9] are based on or derived from the model of Fischer [2]. This allows for an accurate calculation of the effective surface recombination velocity in open-circuit conditions, which might not be accurate at maximum power point. Other models are based on numerical simulations or on calculation spreadsheets [5-8]. They have the advantages to be more accurate than the analytical solutions, but this higher degree of accuracy is paid for by longer computing time, license costs, potentially reduced understanding and the precious time of the best experts. In contrast, suitable, simple, widely applicable and accurate analytical expressions on the other hand would embrace all possible solutions within a few formulae.

The goal of many of the analytical models [2-4] of the PERC solar cell is to replace the structured rear surface by an effective rear surface that is characterized by two parameters: the effective surface recombination velocity ($S_{eff}$) for the rear surface, and an external series resistance ($R_{S\_rear}$) which accounts for the resistance in the bulk. The first goal of this paper is the comparison of the values of $R_{S\_rear}$ and $S_{eff}$ resulting from an earlier published analytical model [4] with its counterpart obtained from three-dimensional (3D) and two-dimensional (2D) numerical simulations.

The $R_{S\_rear}$ and $S_{eff}$ obtained need to be implemented in a separate one-dimensional (1D) model (for example Pitchmaster [10], PC1Dmod [12]), in order to model a solar cell. It is often assumed implicitly that this multidimensional problem (2D or 3D) is equivalent to a one dimensional problem with an effective rear; however it has never been verified to be valid. The second goal of this paper is to verify that this method works. Therefore $S_{eff}$ and $R_{S\_rear}$ are use as parameters of a 1D numerical simulation to model the solar cell. The efficiency obtained is then compared to the one directly obtained from the 3D and 2D simulations.

## 2 MODEL AND SIMULATION

### 2.1 Approach

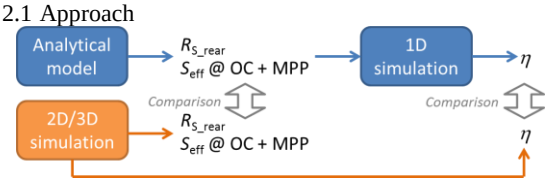


**Figure 1:** Schematics of the approach use to compare the analytical models and the numerical simulations.

In the schematics Figure 1, the steps followed in this paper are represented visually. First, 2D and 3D numerical simulations are carried out in a range of parameters that is technologically relevant. The two parameters representing the rear surface $R_{S\_rear}$ and $S_{eff}$ are extracted from these simulations by analysing the 2D and 3D information about Joule heating due to local currents and the rear surface recombination rate, respectively. The same simulations were also used to obtain the energy conversion efficiency ($\eta$) of these virtual solar cells.

Then, $R_{S\_rear}$ and $S_{eff}$ are calculated using the analytical models. In order to obtain the efficiency, a 1D simulation was carried out using the $R_{S\_rear}$ and $S_{eff}$ values obtained previously. Finally, the analytically and numerically calculated values of $R_{S\_rear}$, $S_{eff}$ and $\eta$ are compared.

### 2.2 Analytical model

The model of Saint-Cast [4] is used in order to analytically calculate the spreading resistance ($R_{S\_rear}$). This model solves the Poisson Equation for point- and

line-shaped contacts assuming a constant current on the front side of the solar cell. This boundary condition should be more suitable for solar cells than a constant voltage on the front considering the homogenous light generation close to the front surface. For contact fractions lower than 10% a simplified formula obtained by parametrisation of the analytical model [9] is available. For line contacts the formula is the following:

$$R_{S\_rear} = \frac{a}{\sigma}\left\{\left(37f - 2 - \frac{0.3}{f}\right) + \frac{2.82w^{0.88}\times f^{0.64}}{\tanh\left(2.82w^{0.88}\times f^{0.64}\right)}\frac{1}{3w}\left(\frac{1}{f}-1\right)^2 + w\right\}$$

and for point contacts:

$$R_{S\_rear} = \frac{a}{\sigma}\left\{\left(2.6 - \frac{0.9}{\sqrt{f}} + \frac{0.24}{f}\right) + \frac{f^{0.25}}{\tanh\left(2w\times f^{0.25}\right)}\frac{-f^2+4f-3-2\ln(f)}{4\left(1-\sqrt{f}\right)f} + w\right\}$$

where $a$ is the contact half width or radius, $f$ is the contact fraction, $w$ is the wafer thickness divided by $a$ and $\sigma$ is the wafer conductivity.

For the analytical modelling of the recombination at the local rear contacts, the model published in Ref. 9 is chosen here. This model is close to the model by Fischer [2]. For the cases of this study only a relatively small difference with Fischer's model has been noticed. The model used here is more general than the one by Fischer and gives a higher accuracy in the case where the contact recombination is not strongly dominating the overall rear recombination [4]. The model is valid for open circuit (OC) condition as no majority current is considered in this model [9] (as for Fischer's model [2]).

The formula used for the calculation is the following [9]:

$$S_{\text{eff}} = \frac{f\times S_{cont} + (1-f)\times S_{pass} + f(1-f)S_{cont}S_{pass}qR_{diff}}{1 + f(1-f)qR_{diff}\left(f\times S_{pass} + (1-f)\times S_{cont}\right)}$$

where $S_{\text{cont}}$ and $S_{\text{pass}}$ are the recombination velocity at the contact and the passivation, $f$ is the contact fraction, $q$ is the electron charge and $R_{\text{diff}}$ is the diffusion resistance of the minority carriers between the contact and the passivation. An analytical calculation for $R_{\text{diff}}$ in the case of line and point contacts can be found in Ref. 9.

2.3 Simulation

For this study the numerical simulations are carried out using a state-of-the-art finite-element software, Sentaurus Device [11]. A large set of parameters is varied in order to obtain a sample which is relevant for applicable technologies. These parameters are listed in Table I. Apart from the parameters reported in this table all the other parameters setting up the simulation are the same, the value of $S_{\text{pass}}$ was 10 cm/s for all simulations. The semiconductor model, the optical model, the emitter, the external resistance are the same for all the simulations regardless whether it is a 1D, 2D or 3D simulation. This insures a consistency within the whole simulation data set under study. The main possible inconstancy which might remain is related to meshing issues, which might affect the results when changing the contact geometry.

**Table I:** Parameters varied in the numerical simulation. For the evaluation of the series resistance, only those setups with a metal fraction below 10% are considered. SRV stands for surface recombination velocity.

| Parameter | Range | # steps |
|---|---|---|
| **Point contact (3D simulation)** | | |
| Contact distance | 0.2-0.6 mm | 7 |
| Contact diameter | 20-80 µm | 3 |
| Contact SRV | $10^2$-$10^4$ cm/s | 5 |
| Bulk resistivity | 1-3 Ω cm | 3 |
| Total | | 315 |
| **Line contact (2D simulation)** | | |
| Contact distance | 0.4-2 mm | 5 |
| Contact width | 30-100 µm | 3 |
| Contact SRV | $10^2$-$10^4$ cm/s | 5 |
| Bulk resistivity | 1-3 Ω cm | 3 |
| Total | | 180 |
| **1D simulation** | | |
| External resistance | 0.5-2 Ω $cm^2$ | 16 |
| Effective rear SRV | 10-$10^4$ cm/s | 74 |
| Bulk resistivity | 1-3 Ω cm | 3 |
| Total | | 3552 |

As explained in the last section, the purpose of the 1D simulations is different from the one of the multidimensional simulations. The 1D simulations are used to obtain the solar cell simulation based on the effective rear parameters $R_{S\_rear}$ and $S_{\text{eff}}$. However, instead of running a new simulation for each parameter calculated in this study, a map of efficiency is created (see figure 2) with more and 1000 points for each bulk resistivity. The efficiency for a specific $R_{S\_rear}$ and $S_{\text{eff}}$ parameters couple is determined by a geometrical mean of the four nearest points.

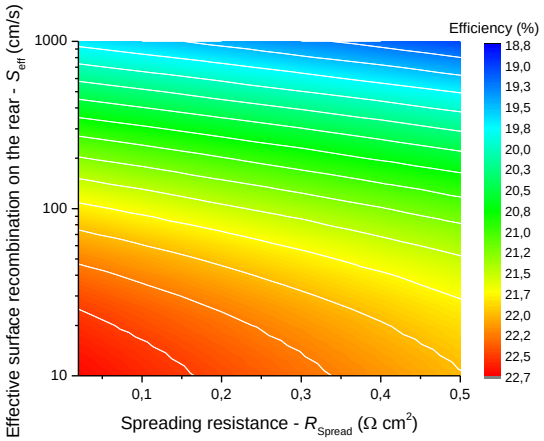


**Figure 2:** Efficiency density plot as a function $R_{S\_rear}$ and $S_{\text{eff}}$ parameters. The efficiency values were obtained from 1D simulation for a bulk resistivity of 1 Ω cm.

## 3 RESULTS AND DISCUTION

### 3.1 Comparison of $R_{S\_rear}$ and $S_{eff}$

In Figure 3, the relative difference between the spreading resistance ($R_{S\_rear}$) obtained by the numerical simulation and the analytical model is presented. As the numerically simulated results are considered to be the reference, this difference between the simulation and the analytical model, will be in the rest of the paper referred as "the deviation" (the deviation of the analytical model from the simulation). The deviation is expressed as the relative deviation. A positive deviation means that the analytical $R_{S\_rear}$ value is higher than its simulated counterpart. The analytical model seems to be in a very good agreement with the simulation. More than 95% of the data shows an deviation below ± 10%.

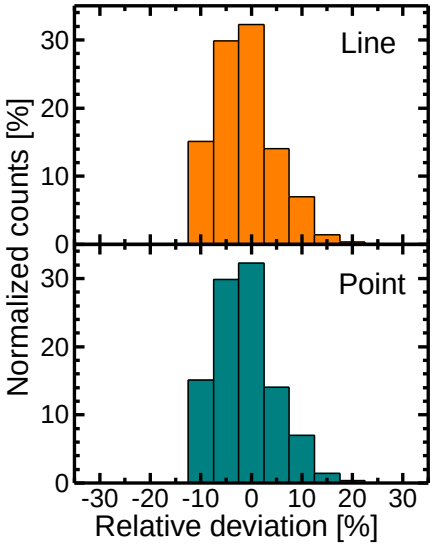


**Figure 3:** Histogram of the deviation for the spreading resistance model for line contacts and point contacts. As mentioned in section 2.2 the $R_{S\_rear}$ model is only valid for a metal fraction below 10%, therefore only the result in this range are compared here

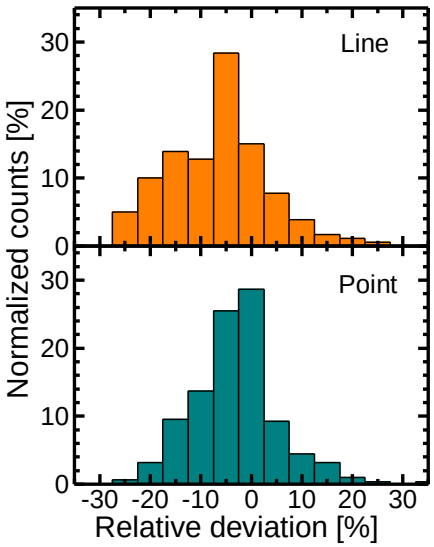


**Figure 4:** Histogram of the deviation for the effective rear surface recombination velocity ($S_{eff}$) for line contacts and point contacts in open-circuit conditions.

In Figure 4, the relative deviation of the effective rear surface recombination velocity ($S_{eff}$) obtained by the analytical model is presented. For this comparison we have chosen to use the values simulated in open-circuit conditions, as in fact the analytical model considers no current flow for its calculation. The analytical model seems to be in a fairly good agreement with the simulation. 94% of the calculated points show an deviation below ± 20% for the line shape contact and below ± 15% for the point shape contacts. An deviation of 20% might look important, but please consider that the recombination rate impacts the voltage only logarimically. Therefore even in the case where the cells' recombination would be largely dominated by the rear surface recombination, the deviation on the open-circuit (OC) voltage would be only about 5 mV.

### 3.2 $S_{eff}$ at the maximum power point (MPP)

The comparison of the $S_{eff}$ provided in open-circuit condition would be sufficient only if it can be shown that the $S_{eff}$ is independent from the working point of the solar cell. However this is not the case. In fact, the $S_{eff}$ obtained by simulation is different under OC as the one under MPP condition. When comparing the $S_{eff}$ obtained analytically with the $S_{eff}$ obtained by simulation in MPP condition only 50% of the points show an deviation less than ± 20%, with a clear tendency to be overestimated (Figure 5).

This change in $S_{eff}$ over the current-voltage characteristics of the cell can be attributed to the majority carrier current flow. In order to understand this more in detail, we need to start from the definition of $S_{eff}$. As defined in Ref. 4, $S_{eff}$ is the average of the local surface recombination velocity (SRV) weighted by the local minority carrier density. Therefore in a defined structure (with a geometry and SRV) the $S_{eff}$ can only change due to a change in the minority carrier distribution. In the analytical models used so far [4,9], it is supposed that the minority carrier distribution only depends on the structure's geometry and the local SRV value; the majority carrier flow is not considered in these models. The majority carrier current is subject to series resistance. This induces an increase of the potential at the *pn* junction, and therefore an increase of the minority carrier density. This increase mainly occurs far from the rear contact, as current flowing laterally over longer distances encounters more series resistance. Therefore it is expected that the series resistance in the bulk or $R_{S\_rear}$ induces an increase of minority carrier density above the passivated area. Following our definition of $S_{eff}$, the weight factor of the SRV on the passivation ($S_{pass}$) needs to be multiplied by the factor $\exp(R_{S\_rear}\, j / V_{th})$, where $j$ is the majority current and $V_{th}$ is the thermal voltage. This leads to an $S_{eff}$ depending on $j$, which can be expressed as follows,

$$S_{eff}(j) = \frac{S_{eff}(0) - S_{pass}}{e^{jR_{S\_rear}/V_{th}}} + S_{pass}.$$

This correction is applied to the value obtained analytically for OC condition (which became $S_{eff}$ (0)) in order to obtain the maximum power point values. In Figure 5 the corrected and uncorrected $S_{eff}$ are compared to $S_{eff}$ obtained from the numerical simulation at the maximum power point (MPP). After correction a fair agreement is obtained with 95% of the calculated points

showing an deviation less than ± 20%.

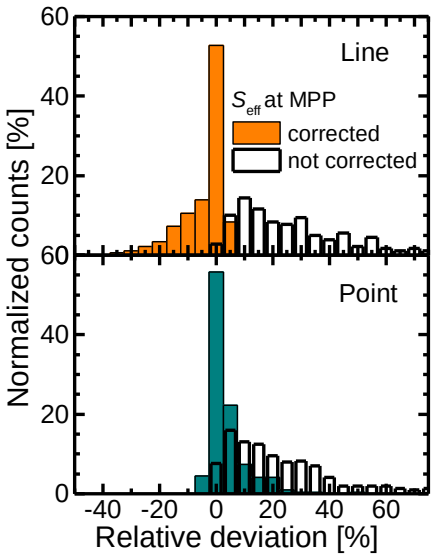


**Figure 5:** Histogram of the deviation for the effective rear surface recombination velocity ($S_{eff}$) for line contacts and point contacts in MPP conditions. The empty bars represent the deviation for the uncorrected $S_{eff}$ and the colored histograms represent the deviation for the corrected $S_{eff}$.

3.3 Comparison of the efficiencies

The efficiency reference values are the ones obtained from the 2D and 3D simulations (for this part the full set of data was used including $f > 10\%$). They are compared to the efficiencies obtained from the 1D simulations using $R_{S\_rear}$ and $S_{eff}$ as inputs parameters. Several $R_{S\_rear}$ and $S_{eff}$ as inputs parameters might be used, we choose to focus on the following scenarios I, II and III:

I. The analytical $R_{S\_rear}$ value and the analytical $S_{eff}$ corrected for MPP condition.
II. The analytical $R_{S\_rear}$ value and the analytical $S_{eff}$ for OC condition, in order to evaluate the gain of accuracy obtained by the correction.
III. The $R_{S\_rear}$ and $S_{eff}$ values obtained by the simulation, which will allow to check the accuracy of the method as we are using or reference values for $R_{S\_rear}$ and $S_{eff}$.

In Figure 6, the histogram or the deviation of the efficiency is presented. In this case the deviation is express directly as the deviation in efficiency in percent absolute.

For the point contacts, we observe a clear gain in accuracy thanks to the correction at MPP condition (scenario I), where more than 96% of the points present an deviation in efficiency of less than $\pm 0.15\%_{abs}$. The efficiencies obtained using $R_{S\_rear}$ and $S_{eff}$ obtained by the 2D/3D numerical simulation (scenario III) are hardly more precise and present a very similar deviation distribution. This suggests that in this case the main source of deviation does not emanate from the analytical model but rather from the method used or the computation accuracy.

Concerning the line shaped contacts, the deviation distribution is much narrower for the values corrected for MPP conditions (scenario I). However, a shift toward higher efficiency is observed in this case. Is seems that the obtained efficiencies are biased by about + 0.15%. A similar bias is observed for the efficiencies obtained using the $R_{S\_rear}$ and $S_{eff}$ values obtained by the 2D/3D numerical simulation (scenario III). This suggests again that the main source of deviation comes from the method used or the computation accuracy. This method might be more suited for the point contact geometry than for the line geometry, but this reason in not understood yet. Another possible explanation might be that the structure of the mesh which varied between 2D and 3D simulation has a unwanted influence.

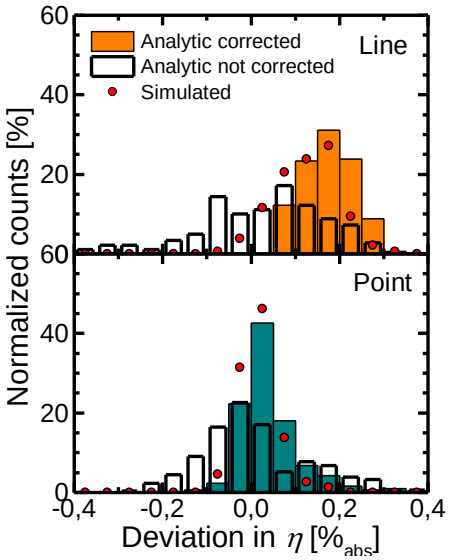


**Figure 6:** Histogram of the deviation for the efficiency by the 1D simulation. The coloured columns are for the analytical $R_{S\_rear}$ values and the analytical $S_{eff}$ value corrected for MPP (scenario I). The empty columns are for the analytical $R_{S\_rear}$ value and the analytical $S_{eff}$ value for OC condition (scenario II). The points are for $R_{S\_rear}$ and $S_{eff}$ values determined from the numerical 2D/3D simulations (scenario III).

## 4 CONCLUSION

This work investigated the accuracy of analytical models for local rear contacts of PERC/PERL solar cells, by confronting them to numerical simulation. The deviation made in the calculation of the series resistance $R_{s\_rear}$ and the effective surface recombination velocity $S_{eff}$ is small enough for most of the practical applications if the parameter range of the model's validity is not left. There is a great confidant that the deviation for $R_{S\_rear}$ is smaller than ± 10% and that the deviation for $S_{eff}$ is smaller than ± 20% for open-circuit conditions. The study of the simulation results shows that $S_{eff}$ varies significantly with the solar cell working point. A correction has been proposed for $S_{eff}$. This correction maintains the same level for accuracy in maximum power point (MPP) conditions.

The correction of $S_{eff}$ does not only increase the accuracy in MPP condition but also the accuracy of the efficiency obtained using 1D simulations to model the solar cell. This method insures with a confidence of 95% that the deviation in efficiency will not exceed $\pm 0.18\%_{abs}$ for point contact and $\pm 0.28\%_{abs}$ for line contacts. The difference between the accuracies for line contact compared to point contact stills needs to be investigated.

## 5 REFERENCES


[1] A. W. Blakers, A. Wang, A. M. Milne, J. Zhao and M. A. Green, Applied Physics Letters, 55(13), 1363–1365 (1989).

[2] B. Fischer, PhD Thesis, University of Konstanz, 2003.

[3] H. Plagwitz, R. Brendel, Progress in Photovoltaics: Research and Applications 2006; 14: 1–12.

[4] P. Saint-Cast, *et al.* Journal of Applied Physics 2010; 108: 013705-013705-013707.

[5] A. Cuevas, IEEE Journal of Photovoltaics 2012; 2: 485–493.

[6] A. Cuevas, JH. Petermann, IEEE Journal of Photovoltaics 2013; 3: 587–589.

[7] A. Cuevas, Journal of Applied Physics 2013; 113: 164502.

[8] A. Cuevas, D. Yan, F. Haasse, J. Petermann, R. Brendel. Energy Procedia 2013; 38: 13–21.

[9] P. Saint-Cast, PhD Thesis, University of Konstanz, 2012. Chapter 2, p.15-70

[10] A. Wolf, D. Biro, J. Nekarda, S. Stumpp, A. Kimmerle, S. Mack, and R. Preu, J. Appl. Phys. 108, 124510 (2010)

[11] Sentaurus Device User Guide, Version H-2013-03. Synopsys, Inc.: Mountain View, CA, 2013.

[12] H. Haug, J. Greulich. "PC1Dmod 6.2–Improved simulation of c-Si devices with updates on device physics and user interface." Energy Procedia 92 (2016): 60-68.